

# Context Preserving Focal Probes for Exploration of Volumetric Medical Datasets

Yanlin Luo, José Antonio Iglesias Guitián, Enrico Gobbetti, and Fabio Marton

CRS4, Pula, Italy

{yanlin,jalley,gobbetti,marton}@crs4.it

**Abstract.** During real-time medical data exploration using volume rendering, it is often difficult to enhance a particular region of interest without losing context information. In this paper, we present a new illustrative technique for focusing on a user-driven region of interest while preserving context information. Our focal probes define a region of interest using a distance function which controls the opacity of the voxels within the probe, exploit silhouette enhancement and use non-photorealistic shading techniques to improve shape depiction.

## 1 Introduction

Visualization and exploration of volumetric datasets coming from MRI or CT scans, both widely used in the medical field, is a very well established research area in Computer Graphics. In the last few years, GPU-based implementations of Direct Volume Rendering (DVR) have emerged as a suitable solution for real-time interactive rendering on desktop platforms [1]. Current solutions are principally based on ray-casters and have demonstrated the capability to manage in GPU moderate-size datasets. Recent results on out-of-core techniques have shown how it is possible to overcome the limitations due to higher resolution datasets [2] [3].

Even though DVR is the most widely used and accepted technique to produce high quality images, there still exist some open issues regarding how to extend its adequacy for the abstraction of significant features from the resultant images, in particular for applications involving clinical diagnosis or medical education. Nowadays non-photorealistic and illustrative techniques are emerging in order to create a new higher layer of abstraction providing us new valuable information.

Our understanding of complex datasets is principally based on structure recognition, and our visual system reduces presented information through abstraction [4]. Therefore, we should equip medical visualization systems with a filtering mechanism for helping us in the task of efficiently abstracting the information of volumetric datasets for better understanding and analysis.

The main control mechanism when using DVR is the specification of colors and opacities. Assigning a high opacity value to a certain portion of the data may result in the occlusion of interesting structures. Furthermore, many overlapping structures may not embody the important structural details, and, in general, cluttered images are quite difficult to understand. Therefore, the challenge is the resolution of the inherent occlusion problem and particularly how to focus and enhance the rendering on a particular region of interest.

Looking into human mental models, we know that the visual information gathering is not a continuous process. The human eye is capable of performing from two up to five fixations per second [5], and gathering and processing of information only occurs during an eye fixation. The eyes rest on a point of the stimulus while the focused information is visually gathered and processed [6]. A motion in the human visual field periphery causes an eye reflex by which an observer focuses on a moving object, differentiating three basic categories of motions in the three-dimensional space: translation, rotation and change of an object's shape [7].

A reasonable idea is, thus, to emphasize our region of interest by decreasing the weight of other parts which can create an occlusion effect or disturb our attention. In this paper, we present a context-preserving enhancement technique based on a focal probe model for exploring volumetric medical datasets. In our model the region of interest is defined by a distance-based function which decreases the opacity of the voxels far from the center, enabling the context-preserving effect. The presented model allows the user to translate, rotate or scale the probe according to the requirements of the region of interest. The probe guides the viewer's attention to its focus region where traditional DVR combined with illustrative techniques are used in order to render and enhance volumetric shapes.

The paper is structured as follows. In Sec. 2 we introduce GPU-based approaches for DVR, as well as non-photorealistic illustrative techniques and context-preserving volume rendering. In Sec. 3, we describe our context-preserving model based on focal probes presenting rendering results in the Sec.4 and conclusions in Sec.5.

## 2 Related work

GPU accelerated volume rendering has become a very well established research area. We refer the reader to the recent book of Engel et al. [1] for a survey on GPU volume rendering. In order to solve the problems due to higher resolution datasets we employ an out-of-core based approach which is based on the management of a hierarchical multiresolution structure in conjunction with adaptive loaders. For a deeper survey on our volume rendering core technology we refer the user to the recent publication of Gobbetti et al. [2].

Our approach to efficiently abstract significant features from the resultant images coming from DVR and its GPU-based implementations, fits within the framework of illustrative visualization.

Traditional illustrative non-photorealistic rendering techniques typically mimic the style of traditional illustrations. They take advantage of the illustrators long experience in depicting complex structures or shapes in an easily comprehensible way. Ebert et al. [8] combine some physics-based illumination model with non-photorealistic techniques to enhance the perception of structure, shape, orientation, and depth relationships in a volume model. For similar purpose, different stylistic choices have been used in traditional medical illustrations, such as silhouette or contour enhancement, pen-and-ink, stippling, hatching, etc. For example, Treavett et al. [9] describe algorithms based on pen-and-ink illustration which are integrated within a traditional volume rendering pipeline. Lu et al. [10] develop a direct volume illustration system that simulates tra-

ditional stipple drawing. Nagy et.al [11] give an approach combining line drawings and direct volume rendering. Dong et al. [12] introduces volumetric hatching directly produced from medical volume data.

In this work, we are interested in techniques for emphasizing details of structures which are in focus and for reducing clutter while preserving useful context information in nearby areas.

Context preserving volume rendering focuses on solving the problem of which part of the volume must be emphasized, and what kind of rendering style is more suitable to enhance this part. At the same time, it faces the problem of how to avoid the collateral effects of losing important context information, maintaining enough visual cues for de-emphasized or less important parts. The main approaches generally rely on exploiting a way to decrease the importance of the less relevant information in favour of a region of interest. Hauser et al. [13] propose the two-level volume rendering model allowing visualization of volume data with important inner structures together with semi-transparent outer parts as context information. They integrate different rendering modes and compositing types, such as DVR, MIP, or tone shading for the inner part of the volume and contour enhancement for the outer part. Cohen et al. [14] discuss in depth how information visualization ideas can be applied to scientific visualization in an effective way. In particular, they combine the “focus and context” concept with distortion effects to improve understanding of large volume datasets. Viola et al. [15] introduce importance-driven volume rendering, where the emphasis can be automatically put on the part which has been assigned more importance. Ropinski et al. [16] propose volumetric lenses to interactively focus regions of interest, rendering the parts of the volume intersecting the lens, which is defined by a convex 3D shape, using a different visual appearance. Bruckner et al. [17] suggest to use cut-away views to focus the attention on the intersection region and ghosting views which tends to generally give a better impression of the spatial location of the object in focus.

Context-preserving in volume rendering can be also achieved by exploiting lighting intensity as an input to a function for opacity variation. Bruckner et al. [18] use this idea to reduce the opacity in rather flat regions oriented toward the light source. Parts of the volume receiving less lighting are rendered as semi-transparent silhouettes helping to preserve context information. Krüger et.al [19] present a method which enables the user to focus on a particular region, using defined parameters such as the size and location of the focus, a weight for the context, and material properties. An approach similar to ours is the one proposed by Zhou et. al [20], which emphasizes a region according to the Euclidean distance from the sampled voxel to a sphere center. Tappenbeck et al. [21] employ distance-based transfer functions, which allows to hide, emphasize or color structures based on their distance to a relevant reference structure. In our approach, we exploit the pq-distance to give a focus shape consistent with a probe defined by a superquadric function. Furthermore, we propose to combine relief shading techniques for enhancing the focus region with a better shape depiction and silhouette darkening effects. For preserving context information, we use an adaptive voxel dependent transparency and perform the clipping of voxels in regions which can create image clutter.

Silhouette enhancement is typically based on gradient or curvature estimations. Csbfalvi et al. [22] visualize object contours based on gradient information as well as on

the angle between viewing direction and gradient vector using depth-shaded maximum intensity projection. Kindlmann et al. [23] employ curvature along the view direction to achieve illustrative effects, such as ridge and valley enhancement. It is also common in medical illustrations to depict shape or surface details in a way that is inconsistent with physically-realizable lighting model. Inspired by the techniques used in cartography, Rusinkiewicz et al. [24] develop a non-photorealistic rendering strategy based on multiscale local toon shading. Based on it, we develop a non-photorealistic shading model applicable to volume rendering.

### 3 The Context-Preserving Focal Probe Model

In our focal probe model we provide the possibility to interactively define a region of interest composed of a part in focus and its context. The focus and context information are separated by the assignment of different rendering styles, which allow to easily distinguish between the different parts. Nevertheless, the rendering styles can be smoothly blended to provide a more continuous effect.

We define the region of interest using a distance-based function which basically decrease the opacity of the samples according to its distance to the center. The focus rendering style is inspired by relief shading techniques to perform enhancement of shape details combined with a silhouette darkening effect. Meanwhile, the context style performs silhouette detection combined with a view-dependent transparency modulation effect. Finally, we clip all samples before the probe and saturate all samples behind it, in order to avoid cluttering results for rays intersecting the probe.

The presented model allows the user to translate, rotate or scale the probe size according to the requirements for an adequate visualization of the datasets.

#### 3.1 Background

We will briefly describe the ray casting process along one viewing ray for simplicity's sake. We assume a volumetric scalar field as  $f(P) \in R$  ( $P \in R^3$ ), then denote the viewing ray direction by  $V$  and its normalized vector by  $\hat{V}$ . Let  $P_i$  be the  $i$ -th sample location along a viewing ray  $V$ ,  $f_i$  be the data value at  $P_i$ ,  $g_i$  be the gradient at  $P_i$  and  $\hat{g}_i$  be its normalized vector. We denote the gradient magnitude by  $\|g_i\|$ , and the normalized gradient magnitude by  $\|\hat{g}_i\|$ , which is  $\|g_i\|$  divided by the maximum magnitude  $\|g_{max}\|$ . Since the gradient has noise, we filter it using an interpolation function as below

$$w_i = \text{smoothstep}(\|\hat{g}_i\|, g_l, g_h) \quad (1)$$

where smoothstep is a cubic function defined by

$$\text{smoothstep}(t, a, b) = \begin{cases} 0 & \text{if } 0 \leq t < a \\ \left(\frac{t-a}{b-a}\right)^2 \left(-2\left(\frac{t-a}{b-a}\right) + 3\right) & \text{if } a \leq t \leq b \\ 1 & \text{if } b < t \leq 1 \end{cases} \quad (2)$$

Conventional volume rendering DVR uses the front-to-back alpha blending which employs a physically motivated absorption-plus-emission optical model, computing the

accumulated opacity  $\alpha_i^*$  and color  $c_i^* = (r_i^*, g_i^*, b_i^*)$  at step  $i$  with regular increment  $\Delta s = \|P_i - P_{i-1}\|$  along the viewing ray  $V$  as follows

$$\begin{cases} c_i^* &= c_{i-1}^* + (1 - \alpha_{i-1}^*)\alpha_i c_i \\ \alpha_i^* &= \alpha_{i-1}^* + (1 - \alpha_{i-1}^*)\alpha_i \end{cases} \quad (3)$$

where  $\alpha_i$  and  $c_i = (r_i, g_i, b_i)$  are the opacity and color respectively at  $P_i$ , both derived from the transfer function.

The light properties make it possible to enhance objects for a variety of effects. Before accumulating, generally we use the traditional Phong model to perform a shading effect by modifying the color  $c_i$  to be the shaded color  $c_{i,\text{shaded}}$  as below

$$c_{i,\text{shaded}} = \lambda_i c_i \quad (4)$$

where

$$\lambda_i = k_a + \sum_{\text{lights}} k_d (\hat{L} \cdot \hat{g}_i) + k_s (|\hat{H} \cdot \hat{g}_i|)^{k_e} \quad (5)$$

$k_a, k_d$  and  $k_s$  are the ambient, diffuse and specular lighting coefficients.  $\hat{L}$  is the normalized light vector,  $\hat{H}$  is the normalized half-way vector, and  $k_e$  is the shininess constant.

After shading, we denote the opacity at  $P_i$  by  $\alpha_{i,\text{shaded}}$ , which basically follows the same variation as color in Eq. 4. Then we substitute  $c_i$  with  $c_{i,\text{shaded}}$  and  $\alpha_i$  with  $\alpha_{i,\text{shaded}}$  into Eq. 3 performing the normal accumulation process.

### 3.2 Probe Shapes

Medical datasets can capture quite heterogeneous parts of the human body, varying in a wide range of physical dimensions. For a satisfactory exploration of diverse volume datasets we propose to use an exploration tool based on the superquadrics family functions. These functions provide us a flexible and relative simple solution for modelling rounded or sharp corners for a variety of basis geometric shapes (See Fig. 1).

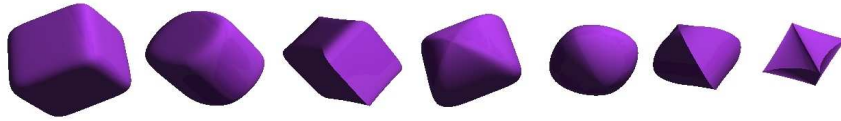


**Fig. 1: Some superquadrics shapes.**

We use a geometric distance based on the pq-norm to define the superquadric. Since it provides us with a distance function, we can use it to define a probe center.

The pq-norm for a sample  $P_i$  with  $x_i, y_i, z_i$  coordinates is defined by

$$\|P_i\|^{pq} = \|(\|(x_i, y_i)\|^p, z_i)\|^q \quad (6)$$

where

$$\|(x_i, y_i)\|^p = (|x_i|^p + |y_i|^p)^{\frac{1}{p}} \quad (7)$$

is p-norm, which is the generalization of the Euclidean metric ( $p = 2$ ). As shown in Fig. 2, various consistent focus shapes can be obtained by using different  $p$  and  $q$  values.

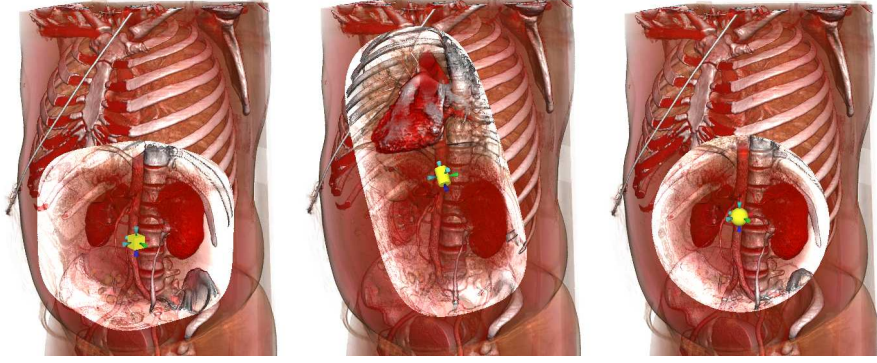


**Fig. 2: Probe shapes.** We have tested various probe shapes, including rounded cubic ( $p = 4, q = 4$ ), cylindrical ( $p = 2, q = 4$ ) and spherical ( $p = 2, q = 2$ ).

### 3.3 Distance based Merging of Rendering Styles

In our focal probe model we propose to employ different rendering styles corresponding with the focus and the context region. One idea could be to use a particular threshold to differentiate between the different zones within the probe, but this decision can lead to sharp transitions with a continuity loss in the resulting rendering. Instead, we propose to merge both rendering styles using a distance-based function  $d_i$  having a plateau for the focus region determined by  $\rho$  ( $0 \leq \rho \leq 1$ ), which can be interactively adjusted by the end user of the system.

$$d_i = \begin{cases} 1 & \text{if } 0 \leq \|P_i\|^{pq} \leq \rho \\ 1 - g_\beta\left(\frac{\|P_i\|^{pq} - \rho}{1 - \rho}\right) & \text{if } \rho < \|P_i\|^{pq} \leq 1 \end{cases} \quad (8)$$

where

$$g_\beta(t) = \frac{t}{e^{\beta(1-t)} + t} \quad (9)$$

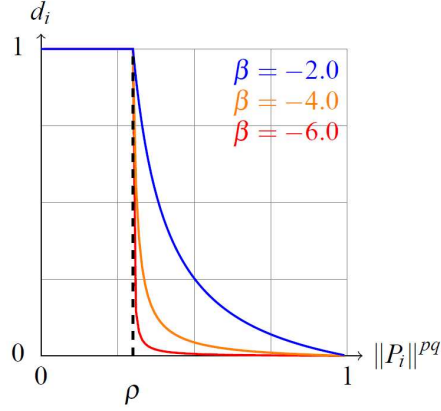


**Fig. 3: Distance based function.**

is the schlick rational function [25]. We use  $\beta$  ( $\beta < 0$ ) for having a smoother or sharper decreasing value of the context region.

We use different rendering styles for the focus and context regions which will be introduced later. Let  $(c_{i,\text{focus}}, \alpha_{i,\text{focus}})$  and  $(c_{i,\text{context}}, \alpha_{i,\text{context}})$  be the color and opacity at  $P_i$  defined by these rendering styles, our proposed blending strategy is performed by using  $d_i$  as focus fraction (See Eq. 10).

$$\begin{cases} c_{i,\text{blend}} = d_i c_{i,\text{focus}} + (1 - d_i) c_{i,\text{context}} \\ \alpha_{i,\text{blend}} = d_i \alpha_{i,\text{focus}} + (1 - d_i) \alpha_{i,\text{context}} \end{cases} \quad (10)$$

After blending,  $c_i$  is substituted by  $c_{i,\text{blend}}$  and  $\alpha_i$  by  $\alpha_{i,\text{blend}}$  into Eq. 3 performing the normal accumulation in the rendering pipeline.

### 3.4 Focus Model

Next, we propose a rendering style which performs better shape depiction for the focus region based on traditional DVR and non-photorealistic techniques (See Fig. 4). In particular, we perform a silhouette darkening effect based on the following detector

$$s_i = w_i * \text{smoothstep}(1 - |\hat{g}_i \cdot \hat{V}|, s_l, s_h) \quad (11)$$

where  $s_l$  and  $s_h$  control the silhouette sharpness. The focus color  $c_{i,\text{focus}}$  and opacity  $\alpha_{i,\text{focus}}$  at  $P_i$  are defined by

$$\begin{cases} c_{i,\text{focus}} = (1 - s_i) r_i c_i \\ \alpha_{i,\text{focus}} = r_i \alpha_i \end{cases} \quad (12)$$

where  $r_i$  is a shading factor implementing an illustrative effect explained next and defined by Eq. 14. We combine the previous color darkening processing with an illustrative relief shading effect. Principles in relief shading [24] advise to omit shadows

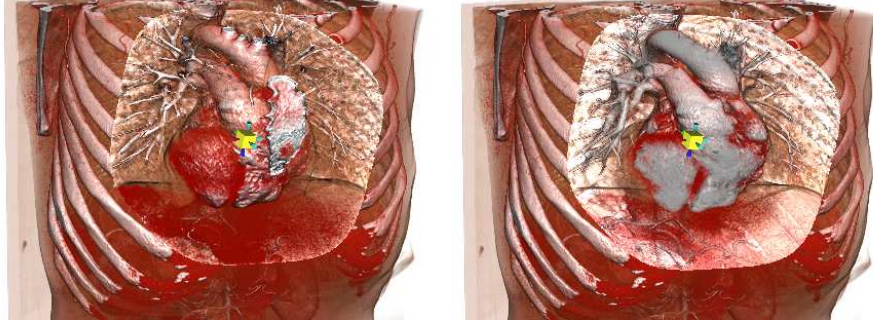


**Fig. 4: Comparison between a probe with and without focus.** On the left image we provide an example of a normal probe without focus. Notice how the sternum bone hides part of the heart. Besides, flesh and lung tissues create a cluttering effect as they cover part of neighbour structures. On the right image, we show the same situation using a context-preserving focal probe. In this case, heart is right focused, no cluttering is created around it. Furthermore, context information is preserved and previously hidden vessel structures are now better identified.

and specular effects, exaggerate the height of ridges and valleys in the object shape and use a particular lighting effect which appears to originate as from the top of the image. Furthermore, these principles suggest to locally adjust light direction in order to homogeneously light the interesting part of the volume. Finally, to support multiscale toon-shading effects, it is recommended to blend between different smoothed versions of the volume.

Applying inside our system Rusinkiewicz et al.'s techniques based on relief shading, requires a special preprocessing to produce smoothed versions of the volume dataset for multiscale-based effects. In our model we will apply similar basis concepts in order for detail enhancement without necessity of preprocessing. We compute on the fly a local version  $\hat{n}_i$  of the smoothed normal, accessing samples located at positions  $x_{i\pm 1}$ ,  $y_{i\pm 1}$  and  $z_{i\pm 1}$  for a sample at  $P_i$  with  $x_i, y_i, z_i$  coordinates. Next, we make a local light adjustment at each sample, computing the new light position  $L_i^*$  at  $P_i$  based on the global light position  $L$ , and the smoothed normal  $\hat{n}_i$  at  $P_i$ . For this purpose, we create a light which is perpendicular to the smoothed normal  $\hat{n}_i$ , exaggerating the shading effect for ridges and valleys in our volume (See Eq. 13).

$$L_i^* = L - \hat{n}_i(\hat{n}_i \cdot L) \quad (13)$$

Furthermore, as shown in Eq. 14, we use the original shading  $\hat{L} \cdot \hat{g}_i$  as a basis for the lighting of the diffuse component, thus to avoid the appearance of excessively dark zones in the final rendering. Next, we sum the contribution of the  $P_i$  local light  $\hat{L}_i^* \cdot \hat{g}_i$ . Finally, we have altered the local lighting to produce a toon shading effect, just clamping  $\hat{L}_i^* \cdot \hat{g}_i$  between 0 and 1 and multiplying the result by the toon shading factor  $a$ .

$$r_i = k_a + k_d(\hat{L} \cdot \hat{g}_i + a * \text{clamp}_{[0..1]}(\hat{L}_i^* \cdot \hat{g}_i)) \quad (14)$$

### 3.5 Context Model

The rendering style proposed for the context region is based on view-dependent transparency and silhouette detection. The context color  $c_{i,\text{context}}$  and opacity  $\alpha_{i,\text{context}}$  at  $P_i$  are defined by

$$\begin{cases} c_{i,\text{context}} = \lambda_i c_i \\ \alpha_{i,\text{context}} = h(\theta) s_i \lambda_i \alpha_i \end{cases} \quad (15)$$

where

$$h(\theta) = \begin{cases} 0 & \text{if } 0 \leq \theta \leq \varphi \\ 1 - \frac{\cos\theta - \cos\varphi}{\cos\phi - \cos\varphi} & \text{if } \varphi < \theta \leq \phi \end{cases} \quad (16)$$

Shown by the left most image in Fig. 5,  $\theta$  is the angle formed by the  $O$  vector connecting the eye position with the probe center and the viewing direction  $V$ ,  $\phi$  is the angle defining the maximum angle for rays intersecting the probe, and finally  $\varphi$  the angle defining rays passing through the focus region. The shading factor  $\lambda_i$  has been previously defined by Eq. 5. The  $\alpha_{i,\text{context}}$  parameter introduces a view-depnt effect, giving more opacity to voxels in the outer part of the probe and increasing the transparency as samples are closer to the probe center.

The use of volumetric probes entails the problem of possible occlusion due to the voxels situated between the eye position and the probe. This is also valid for voxels in the context region, which can impede the correct visualization of our interest region. We illustrate this problem in the right image of Fig. 5. Therefore, a reasonable strategy seems to cancel the accumulated color just before the first intersection of the viewing ray with the probe, corresponding to the red cone in the right of Fig. 5. Samples in the context region behind the probe focus are ignored, and following samples in the volume are blended with the background contributing less to the final accumulated color along the ray.

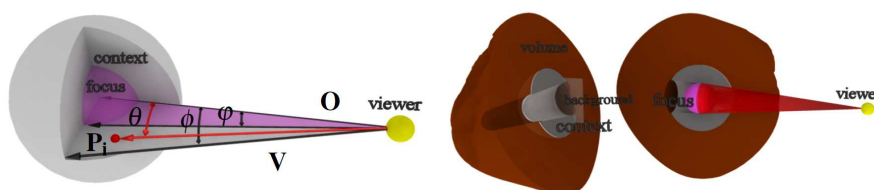


**Fig. 5: Context definition for focal probes** In the left image, for a sample  $P_i$  in the context region, we define the  $\theta$  angle which decides how much the context will be displayed. In the right, voxel clipping is performed in order to produce a non cluttered render image.

## 4 Results

We report on the results obtained when performing exploration of medical datasets by using our focal probe model. We have tested the proposed technique with a variety of volumetric medical datasets. We discuss the results obtained with the inspection of a  $512 \times 512 \times 1559$  whole body contrast and a  $512 \times 512 \times 743$  torax study, both CT <sup>1</sup> with *16bit/sample*.

Regarding the focal probe model, we employ the following parameter configuration. We use  $\beta = -2.0$  for having a smooth transition between the focus and context information (See Fig.3). To separate the focus and context regions, we adjust the  $\rho$  parameter in the interval  $[0.4, 0.7]$ . For gradient filtering we compute the  $w_i$  interpolation function with  $g_l = 0.015$  and  $g_h = 0.95$ . Related with the non-photorealistic shading, we control the silhouette detector  $s_i$  using  $s_l = 0.7$  and  $s_h = 0.95$  for a fine silhouette enhancement without creating cluttering owing to low gradient values. We define the toon shading factor  $a = 3.0$  to enhance lighting differences between ridges and valleys in the focus region.

As described in Fig. 3 the behaviour of our focal probe model establishes a center of attention, fitting in the region around of the probe center. Transparency is modulated by the  $d_i$  distance based function and its effect results in more transparency for voxels in the context region. In Fig. 6 we can appreciate the effect of an interactive incursion of a focal probe within the whole human body CT. At the beginning, the probe acts just as a clipping sphere and as soon as the center of the probe is inside the volume, the focus effect becomes visible, as well as the context-preserving effect showing contour shapes. When exploring parts of the volume which are too deep, voxel clipping becomes active.

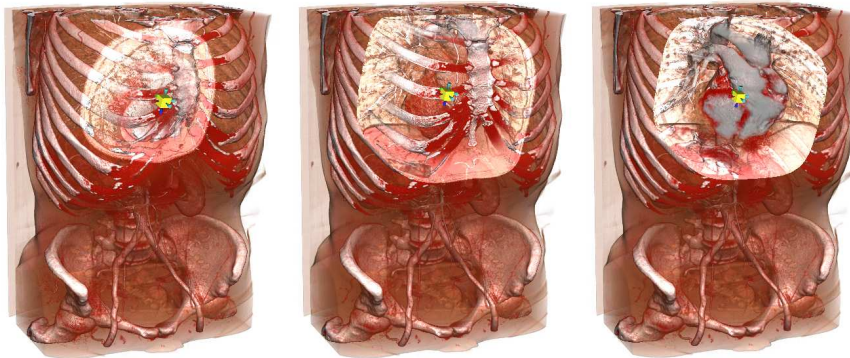


**Fig. 6: Context-preserving focal probe.** From left to right we increase the focal probe penetration stopping when the heart is right focussed in the center of the probe.

Using the silhouette darkening effect we can depict shape borders using a darker color and enhancing the shape over its background. In Fig. 7 we show a series of snap-

<sup>1</sup> Source: Geneva University Hospital, Radiology Department

shots of our volume renderer varying the parameter  $s_h$  of Eq. 11, which indicates the threshold value above which a sample is considered a border shape.

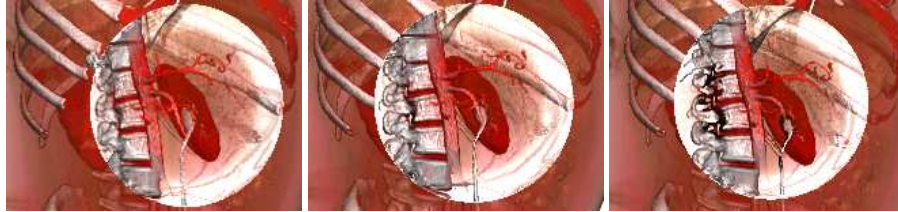


**Fig. 7: Silhouette darkening effect.** From left to right, no silhouette darkening  $s_h = 1$ , silhouette darkening with  $s_h = 0.8$  and  $s_h = 0.4$ .

The relief shading technique, described in Sec. 3.4, allows the user to appreciate additional details within the focus region, exaggerating the lighting effect by using a perpendicular light for each voxel (See Fig. 8). In our approach we rely on a local version of the smoothed normals, and for this reason, the enhanced details are limited to local details, normally corresponding to high frequencies in the volume.

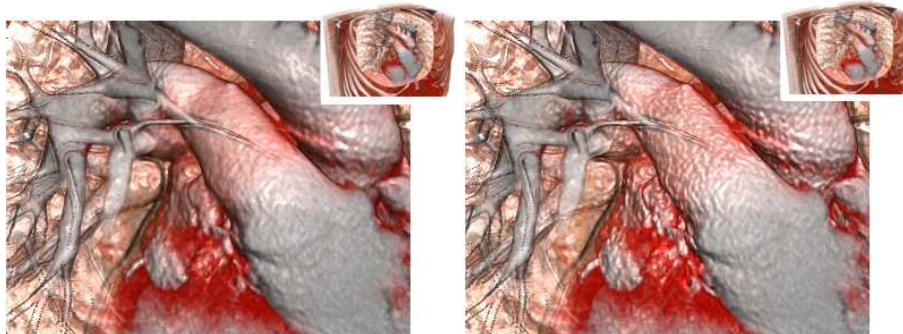


**Fig. 8: Relief shading effect.** On the left we show a probe focus without relief shading. On the right we show the same viewpoint with relief shading for the focus probe. Notice the how high frequency details are highlighted.

## 5 Conclusion

We have described an alternative focal probe model for interactive exploration of medical volumetric datasets. The key feature of our approach relies on the enhancement of natural filtering mechanisms of humans to separate and abstract information.

Our model is based on the development of different rendering styles for the focus and context information. The superquadrics family functions are used to get consistent focus shapes. Furthermore, we propose an adaptive voxel shading, based on illustrative non-photorealistic techniques, in order to enhance shape depiction in the focus region. In addition, we use silhouette detection to convey better structure cues in the focus region and to preserve the context information in the outer part. Finally, we propose a strategy to smoothly blend both rendering styles.

A particular clipping strategy is performed for voxels in front of the probe and behind it, in order to solve the occlusion problem and to avoid the creation of a noisy background.

**Acknowledgments:** This work is partially supported by the EU Marie Curie Program under the 3DANATOMICALHUMAN project (MRTN-CT-2006-035763).

## References

1. Engel, K., Hadwiger, M., Kniss, J., Rezk-Salama, C., Weiskopf, D.: Real-time Volume Graphics. AK-Peters (2006)
2. Gobbetti, E., Marton, F., Iglesias-Gutián, J.A.: A single-pass GPU ray casting framework for interactive out-of-core rendering of massive volumetric datasets. *The Visual Computer* **24**(7–9) (2008) 797–806
3. Crassin, C., Neyret, F., Lefebvre, S., Eisemann, E.: Gigavoxels: Ray-guided streaming for efficient and detailed voxel rendering. In: ACM SIGGRAPH Symposium on Interactive 3D Graphics and Games (I3D). (2009) 15–22
4. Hendee, W.R., Wells, P.N.T.: The perception of visual information. Springer, New York. (1997)
5. Ware, C.: Information Visualization: Perception for Design. Morgan Kaufmann Publishers, San Francisco (Second Edition; 2004)
6. Smolnik, S., Nastansky, L., Knieps, T.: Mental representations and visualization processes in organizational memories. In: Proceedings of the Seventh International Conference on Information Visualization (IV03), Los Alamitos, CA, USA, IEEE Computer Society (2003) 568–575
7. Thomas, R.J., Strothotte, T.: Motion enhanced visualization in support of information fusion. In: Proceedings of International Conference on Imaging Science, Systems, and Technology (CISST2001), Las Vegas, CSREA Press 492–497
8. Ebert, D., Rheingans, P.: Volume illustration: non-photorealistic rendering of volume models. In: Proceedings of IEEE Visualization. (2000) 195–202
9. Treavett, S.M.F., Chen, M.: Pen-and-ink rendering in volume visualization. In: Visualization '00: Proceedings of the 11th IEEE Visualization 2000 Conference (VIS 2000), Washington, DC, USA, IEEE Computer Society (2000)
10. Lu, A., Morris, C.J., Ebert, D.S.: Non-photorealistic volume rendering using stippling techniques. In: Proceedings of IEEE Visualization. (2002) 211–218
11. Nagy, Z., Schneider, J., Westermann, R.: Interactive volume illustration. In: Proceedings of Vision, Modeling, and Visualization. (2002) 497–504
12. Dong, F., Clapworthy, G.J., Lin, H., Krokos, M.A.: Nonphotorealistic rendering of medical volume data. *IEEE Comput. Graph. Appl.* **23**(4) (2003) 44–52
13. Hauser, H., Mroz, L., Bischian, G.I., Gröller, M.E.: Two-level volume rendering. *IEEE Transactions on Visualization and Computer Graphics* **7**(3) (2001) 242–252

14. Cohen, M., Brodlie, K.: Focus and context for volume visualization. In: TPCG '04: Proceedings of the Theory and Practice of Computer Graphics 2004 (TPCG'04), Washington, DC, USA, IEEE Computer Society (2004) 32–39
15. Viola, I., Kanitsar, A., Gröller, M.E.: Importance-driven volume rendering. In: Proceedings of IEEE Visualization 2004. (2004) 139–145
16. Ropinski, T., Steinicke, F., Hinrichs, K.H.: Tentative results in focus-based medical volume visualization. In: Proceedings of the 5th International Symposium on Smart Graphics (SG06). Volume 3638 of Lecture Notes in Computer Science., Springer-Verlag (2005) 218–221
17. Bruckner, S., Gröller, M.E.: Volumeshop: An interactive system for direct volume illustration. In: IEEE Visualization. (2005) 671–678
18. Bruckner, S., Grimm, S., Kanitsar, A., Gröller, M.E.: Illustrative context-preserving exploration of volume data. *IEEE Trans. Vis. Comput. Graph* **12(6)** (2006) 1559–1569
19. Krüger, J., Schneider, J., Westermann, R.: Clearview: an interactive context preserving hotspot visualization technique. Volume 12. (2006) 941–948
20. Zhou, J., Döring, A., Tönnies, K.D.: Distance based enhancement for focal region based volume rendering. In: Proceedings of Bildverarbeitung für die Medizin'04. (2004) 199–203
21. Tappenbeck, A., Preim, B., Dicken, V.: Distance-based transfer function design: Specification methods and applications. In: Proceedings of SimVis 2006. (2006)
22. Csbfalvi, B., Mroz, L., Hauser, H., König, A., Gröller, M.E.: Fast visualization of object contours by non-photorealistic volume rendering. *Computer Graphics Forum* **20(3)** (2001) 452–460
23. Kindlmann, G., Whitaker, R., Tasdizen, T., Möller, T.: Curvature-based transfer functions for direct volume rendering: Methods and applications. In: Proceedings of IEEE Visualization. (October 2003) 513–520
24. Rusinkiewicz, S., Burns, M., DeCarlo, D.: Exaggerated shading for depicting shape and detail. In: ACM Transactions on Graphics (Proc. SIGGRAPH). Volume 25. (2006)
25. Schlick, C.: A fast alternative to phong's specular model. In: Graphics Gems IV, San Diego, CA, USA, Academic Press Professional, Inc. (1994) 385–387